International Journal of Current Engineering and Technology
E-ISSN 2277 – 4106, P-ISSN 2347 – 5161

Available at http://inpressco.com/category/ijcet

Research Article

Structural Morphology and Electrical Properties of Vacuum Evaporated SnS Thin Films

Bushra A.Hasan[†] and Eman M. Nasir[†*]

[†]University of Baghdad, College of science, Physics Department, Baghdad, Iraq

Accepted 22 March 2015, Available online 29 March 2015, **Vol.5, No.2 (April 2015)**

Abstract

Using thermal evaporation technique tin Sulphide (SnS) thin films have been deposited on glass slides have been deposited at room temperature using SnS powder. The deposited films have been investigated through X- ray diffraction measurements to determine structural properties. The deposited SnS films found polycrystalline with an orthorhombic structure. The grain size found to increase with thickness. The surface morphology of the films has been examined using atomic force microscopy AFM. The chemical compositions of the films have been determined using energy dispersive analysis of x-rays (EDAX). The dielectric properties of SnS thin films deposited with different thickness (100,200,and 300nm) are presented in this work. The dielectric permittivity ε and ac conductivity σ_{ac} were measured at temperatures in the range of 293–493 K and frequencies in the range of 10 kHz–100MHz. It is found that there are two conductivity mechanisms and hence two activation energies converts to one mechanism with the increase of thickness. The ac activation energy E_{AC} decreases with increase of thickness and frequency. The exponent s shows a progressive decrease with thickness. The results are explained in terms of structural difference by the effect of thickness and thermal treatment. Few anomalies in dielectric studies were observed near 340 and440K, respectively. These points were related to crystalline phase transitions. Dark-conductivity and photo-conductivity increases with increase of thickness.

Keywords: *SnS semiconductor, XRD, dielectric properties, photoconductivity*

1. Introduction

Tin sulfide (SnS) is an IV-VI binary semiconductor compound whose constituent elements Tin (Sn) and Sulfur (S) are abundant in nature. SnS in its orthorhombic crystalline structure has direct and indirect band gap values between 1.3–1.5 eV and 1.0–1.1 eV, respectively and has p-type conductivity. It has higher absorption coefficient (~10^5 cm^{-1}) compare to other materials like GaAs and CdTe. These properties make it a better alternative absorber material for photovoltaic applications (J. B. Li *et al*, 2012; P. P. Choi *et al*, 2012; J. J. Scragg *et al*, 2012; L. Grenet *et al*,2012). SnS thin films have been deposited by different techniques such as: the vacuum evaporation of the SnS compound (L. Price *et al*, 1999), two stage process (K.T. Ramakrishna *et al*,2002) and electrochemical deposition (Y. Yamazaki *et al*, 2003). In this work, thin films of SnS have been grown by thermal evaporation of the prepared bulk material. A description of the methods used for the growth of the SnS films and details of the effect of the deposition parameters on the a.c conductivity properties as well as on the phase and crystalline structure in which the samples grow, will be reported. Moreover, we present the activation energy value from the temperature-dependent conductivity measurement. An analysis of the published data indicates that little is known about the a.c conductivity of SnS thin films. Because of this reason, an attempt has been made to deposit SnS thin films with different thicknesses at room temperature in the present work. SnS that have been carried out till date, the experimental results on dielectric study are very few, and that too are very less informative. It is well known that dielectric properties of every solid are very sensitive to the local electric field distribution in the sample. Therefore, the temperature and frequency dependence of dielectric constant and loss can explore useful information about structure changes, transport mechanism and defect behavior.

2. Experimental Description

Source material, SnS was prepared by melting high purity elements (99.99%) Sn and S in an evacuated quartz tube at a temperature of 1173 K. Tin sulfide films with different thicknesses (100,200,and 300nm)were deposited on corning 7059 microscopic glass substrate by thermal evaporation technique under high vacuum (10^{-5} Torr) at room temperature.

*Corresponding author: **Eman M. Nasir**

The distance between source and substrates, rate of deposition have been maintained as constant at 15 cm and 8 Å/s, respectively. The as-deposited thin films of SnS were characterized for structural, and dielectric properties. The as-deposited thin films of SnS were characterized for morphology, structural, and optical properties. The composition of the films was estimated using energy dispersive analysis of x-rays (EDAX). The structural studies of the films were carried out using x-ray diffraction (XRD, Model: Philips X'Pert Pro) and structure dependent parameters, namely, crystallite size, microstrain and dislocation density have been evaluated. The surface morphology of the SnS films were examined using AFM at room temperature. The optical transmittance measurements were made in the wavelength range 400-1200 nm, using FT-IR spectrometer. Optical Interference Fringes was used to measure film thickness and Fizaeu fringes of equal thickness are obtained in an optical apparatus of the type ,the film thickness (d) is given by:

$$d = \frac{\lambda}{2}\frac{\Delta x}{x} \qquad (1)$$

Where Δx is the shift between interference fringes. λ is the (Na) wavelength (5893A°) and x is the distance between interference fringes. The samples having almost thickness of about t $\pm$ 10nm.

The prepared thin films were then used for dielectric measurement by coated its opposite faces using high grade conducting layer of Silver paste. The variation of dielectric constant (real and imaginary), loss and ac conductivity with temperature at different frequency (10k Hz-10MHz) was studied from room temperature to 220 ^{o}C using Hewlett Packard model (HP4274A & HP4275A).The results were analyzed and discussed in detail. A thin layer of aluminum electrode was deposited on the SnS thin films for I-V tests. I-V characteristic curves were obtained by a Keithley616.

3. Results and Discussion

A. Surface morphology and compositional analysis

The composition analysis of the SnS films showed that the tin and sulfur content in the films gradually varied with the increase of thickness. The films grown at lower thickness are sulfur rich, whereas films thickness increases was nearly stochiometric. Fig.1 shows AFM micrograph of SnS thin film deposited at three thickness temperatures, 100 , 200and 300nm. AFM images revealed the growth of randomly oriented, worm-like grains, which are uniformly distributed over the surface. From the micrograph it is clearly seen that grain size is increased with increase of Ts, which is clearly observed. The formation of bigger grains is due to coalescence of smaller grains. The average grain size and rms value of surface roughness were found to increase with increase in the thickness. Availability of thermal energy at higher thickness is responsible for increased grain size (L. Price *et al*, 1999). The variation of grain size and surface roughness, with thickness is indicated in Table 1

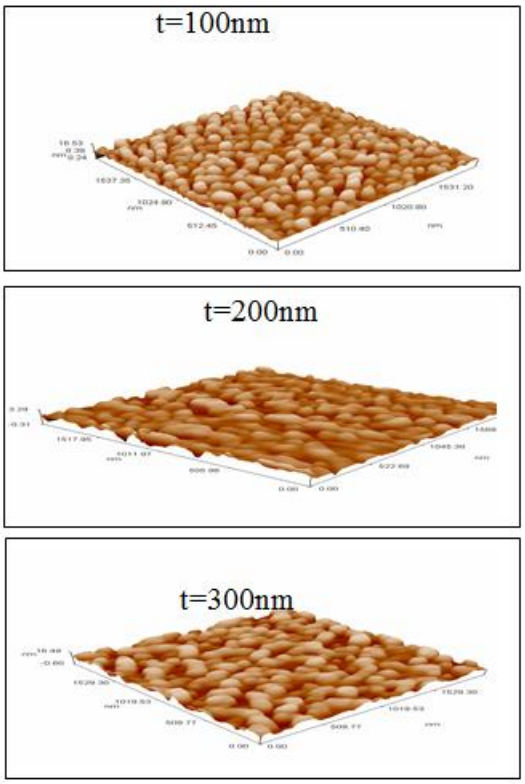

Fig. 1 AFM pictures of SnS thin films deposited with different thickness

Table 1 Average grain size and average roughness for SnS thin films

Thickness(nm)	Average roughness(nm)	Average grain size(nm)
100	2.17	83.24
200	0.348	96.34
300	2.42.4	101.55

B. Structural studies

Fig.2 depicts XRD spectra of SnS thin films deposited at different thickness in the range 100-300nm. The spectra reveal the presence of traces of other phases along with predominant SnS phase. Degree of crystallinity was also found to increase with thickness. The XRD spectra of films grown with lower thickness (t ≤100nm) showed presence of Sn_2S_3 phase, along with dominant SnS phase. The films deposited with t =200nm showed peaks mainly of SnS phase along with minor peaks corresponding to (SnS) phase zinc blend (ZB). No peaks are observed corresponding to SnS_2. However, the films deposited with t = 300nm exhibited only SnS phase. The less intense reflection of the peaks could be due to the presence of other phases in the film while the peak intensity is found to be increased in of sample with thickness 300nm prepared at room

Table 2 Micro structural properties of SnS thin films

Thickness nm	hkl	d(Å) Exp	2 θ	FWHM (β)	Grain Size(D) (nm)	εx10^{-3}	δx10^{15}(lin/m^2)
100	(040) (131)(OR) Sn_2S_3	2.68 2.77 2.56	33.39 32.17 34.49	0.0767 0.0625 0.0867	11.305 13.834 10.025	1.83 1.5 2.07	7.82 5.23 9.95
200	(111)(OR) (120)(ZB) (021)(OR)	2.82 3.38 3.36	31.60 26.29 25.68	0.0733 0.0673 0.0533	11.765 12.673 15.981	1.76 1.63 1.29	7.22 6.23 3.92
300	(111)(OR) (200)(ZB) (101)(OR)	2.83 2.90 2.92	31.55 30.78 30.56	0.0540 ------- 0.0480	15.969 ------ 17.941	1.29 - 1.15	3.92 - 3.11

temperature indicating to the better crystalinty ,specimen broadening intensity arises due to small crystalline (grain) size and strain(lattice distortion). Structural parameters such as crystallite size, strain, lattice parameter, dislocation density were calculated from XRD pattern. The crystallite size of the film was calculated from the Debye Scherer's formula, D = 0.94λ/(β cosθ), where β is the FWHM intensity in radians. The strain and dislocation density values were estimated using following standard relations. Strain (ε) = (β cos θ) / 4, dislocation density $\delta = \frac{1}{D^2}(lines/m^2)$. Crystallite size was increased from 11 nm- 16 nm with increase of thickness. Generally the microstrain is indirectly proportional to crystallite size. It was observed that lattice strain and dislocation density decreased with increase of thickness (Table 2). This is an essential property for the fabrication of good quality thin film to use in optical devices. It is to be noted here that, crystallite size estimated from Scherer's formula is much smaller than the grain size estimated from AFM study. This indicated that grain is made up of several different crystallites.

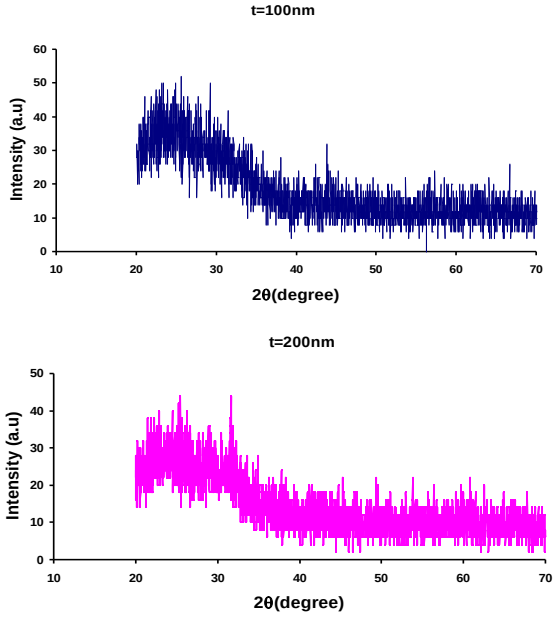

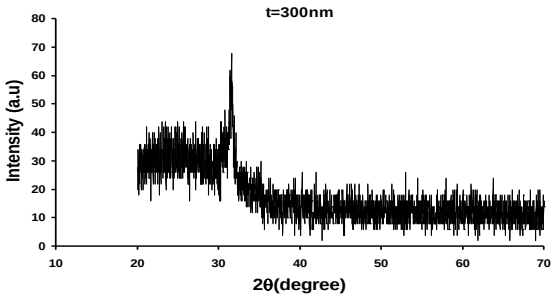

Fig. 2 XRD spectra of SnS thin films deposited at different values of thickness

3.1 Electrical properties of SnS thin films

3.1.1 A.C Conductivity

The ac conductivity can be directly related to the imaginary part of deictic constant ε_i as $\sigma_{ac} = \omega\varepsilon_0\varepsilon_i$ where ε_0 and ω are the permittivity of free space and angular frequency respectively. The variation of ac conductivity with frequency and temperatures (293-493K) of SnS of different thicknesses is shown in Fig.3. A smooth increase in the ac conductivity is observed throughout the temperature for lower thicknesses, while σ_{ac} decreases with temperature for higher thicknesses. The ac conductivity patterns for lower thickness show a frequency independent plateau in the low frequency region and exhibits dispersion at higher frequencies. This behavior obeys the universal power law (A. K. Jonscher , 1983, A.K. Jonscher , 1977), $\sigma(\omega) = \sigma_0 + A\omega^s$ where σ_0 is the dc conductivity (frequency independent plateau in the low frequency region), A is the pre-exponential factor and s is the fractional exponent between 0 and 1.The conductivity spectrum for t=100nm is frequency dependent in the hole frequency range where the deviation from σ_{dc} (plateau region) is more prominent .The increase of thickness the conductivity spectrum differs such that frequency independent plateau expand to high frequency range specially at t= 300nm , however the increase of temperature admonished the independent frequency plateau region . The deviation from σ_{dc}

(plateau region) value in the conductivity spectrum (in the low frequency region) is due to the electrode polarization effect. The values of s were obtained by fitting the $\sigma(\omega) = \sigma_0 + A\omega^s$,s is tabulated in Table1. Generally, power law exponents (s) exceeded unity for t=100 and 200nm. It is found that s value decreases with the increase of thickness indicating the ideal long-range pathways and diffusion limited hopping (tortuous pathway) respectively (K. A. Mauritz, 1989).The value of exponent of the higher frequency slopes (Table-3) shows that the long-range drift of charge carriers may be one of the sources of conduction. From the Table-3, it is clear that the dc conductivity (σ_0) increases with increase in thickness. It is clear that *s value* for t=300nm are less than unity which confirmed the hopping mechanism (K. P. Singh *et al*, 1998).

Table 3 Values of s andα of SnS films

Thicknes s(nm)	Oven Temperature (K)	s	α
100	293	1.055	0.133
	343	1.34	0.277
	393	1.121	0.166
	443	1.028	0.222
	493	0.9757	0.055
200	293	1.055	-
	343	1.34	-
	393	0.838	-
	443	0.6654	-
	493	0.2951	0.444
300	293	0.6229	-
	343	0.3436	0.222
	393	0.2072	-
	443	0.9879	0.1
	493	0.7142	0.244

It is obvious that s decreases for with temperature for lower thicknesses (100,200) nm which makes the correlated barrier hopping (CBH) the most suitable model. The CBH model is adopted when the electrons hop over the potential barrier between two sites; the ac conductivity is due to hopping between defect states or dangling bonds (D^+D^-). In CBH, the $\sigma_{ac}(\omega)$ is exponentially dependent on temperature, while s for t= 300nm decreases with t in the first stage and then increases with increase of *T*; hence small poloran (SP)is the suitable model. When the exponent *s* gets to rise with the increase of temperature for high thicknesses (300nm), this occurs when the addition of the charge carrier to the covalent solid causes a large degree of local lattice distortion, which forms a small polaron (S. Ramesh *et al*, 2002).

The activation energy for conduction (E_a) in the entire region has been shown in figure .4. The values of ac activation energy (E_{ac}) for SnS films were determined from the plot of Ln $\sigma_{ac}(\omega)$ against the reciprocal of Kelvin temperature. E_{ac} were estimated by fitting different regions with the Arrhenius equation $\sigma_{ac} = \sigma_o \exp -\frac{E_a}{kT}$ (B. Natesan *et al*, 2006) and is illustrated in table 4 at selected frequencies (10 kHz, 100 kHz, and1MHz). The data show that each sample reveals two conduction mechanisms. Moreover, the values of E_{ac} decrease with increasing frequency, while the same decreases with thickness. For example, E_{ac} decreases from 0.1004 to 0.0688 eV when the frequency increases from 10k Hz to 100 kHz and while E_{ac} decreases from 0.1004 to 0.1189 eV when *t* increases from 100 to 300nm. The decrease of E_{ac} with the increase of frequency results from the increase of vibrating energy supplied from the increasing frequency of the electric field which causes the decrease of E_{ac} values. This affirms the conductivity is pure ac. The decreases of E_{ac} can be explained as the action of increase grain size.

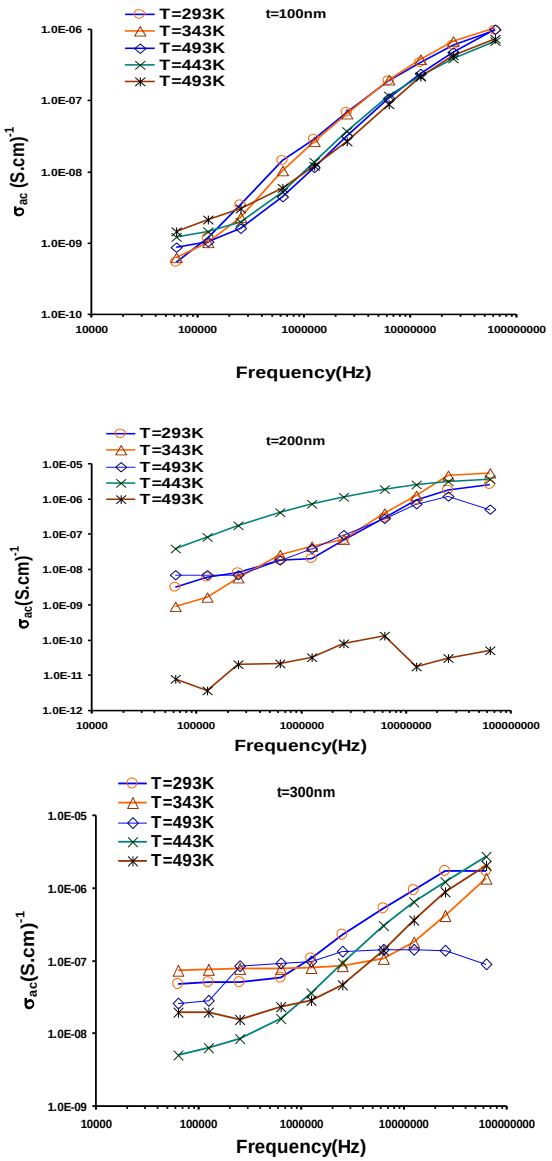

Fig.3 Frequency dependence of AC conductivity for SnS film with different thicknesses and temperatures

Table 4 E_{ac} values of SnS films

Thickness (nm)	F=10kHz		F=100kHz	F=1000kHz
	E_{ac1}(eV)	E_{ac2}(eV)	E_{ac1}(eV)	E_{ac1}(eV)
100	0.153	0.0637	0.0458	0.0193
200	0.146	0.0578	0.0442	0.0177
300	0.094	0.0445	0.0428	0.0164

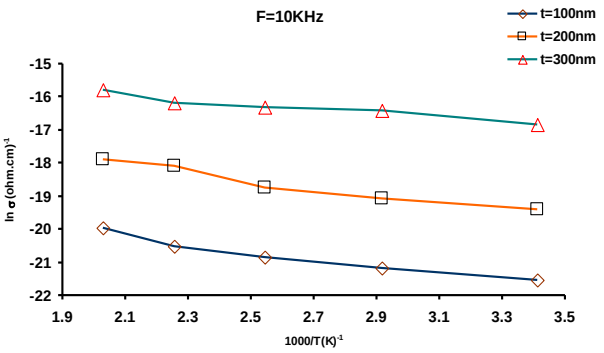

Fig. 4 Plot of ln ac conductivity versus 1000/T characteristics for a film of thickness 100 nm

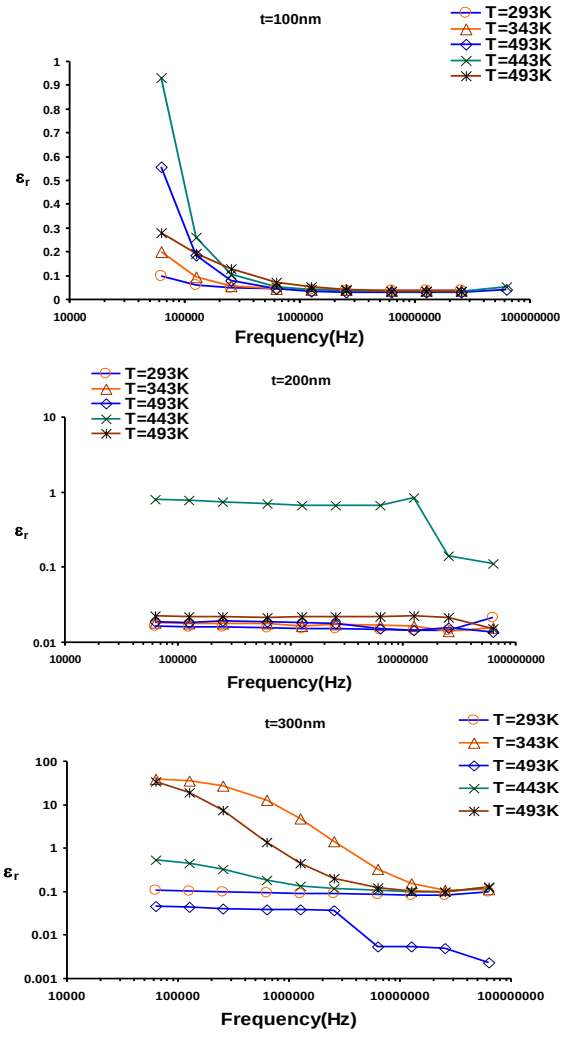

Fig.5 Variation of real part of permittivity (ε_r) with frequency of SnS films with different thicknesses and temperatures

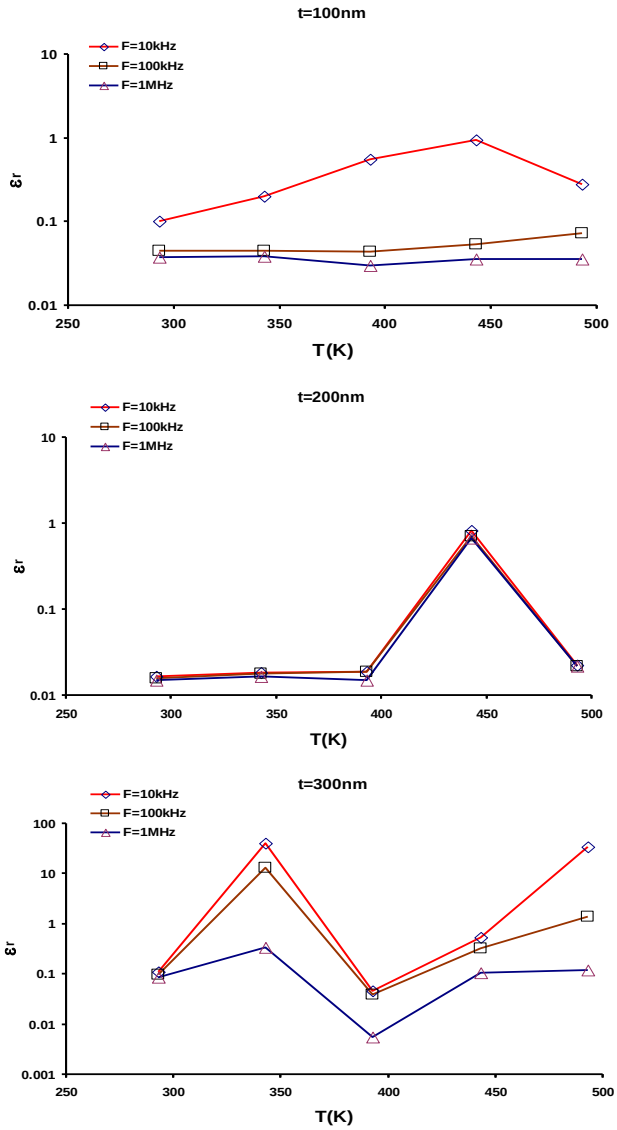

Fig.6 Temperature dependence real part of permittivity (ε_r) for SnS film with different thicknesses at 10 kHz

Fig.5 and 6 show that the variations of ε_r, with frequency for the SnS films having different thickness and at different temperatures respectively. In all the cases, a strong frequency dispersion of permittivity is observed at low frequency region followed by a nearly frequency independent behavior above1000 kHz and 10MHz for t=100 and 200, 300 respectively. The decrease of (ε_r) with increase in frequency may be attributed to the electrical relaxation processes, but at the same time the material electrode polarization cannot be ignored. The material electrode interface polarization superimposed with other relaxation processes at low frequencies. It is seen that with increase of thickness, (ε_r) value increases in the lower frequency and nearly same in the higher frequency region. The thickness increment may result in more localization of charge carriers along with mobile ions causing higher conductivity. This may be the reason for higher (ε_r) and strong low frequency dispersion.

On the other hand the real dielectric constant increases with temperature up 443K but then decreases with further increase of temperature. Indeed ε_r increases from 0.0997 to 0.108 when thickness increases from 100 to 300 nm.

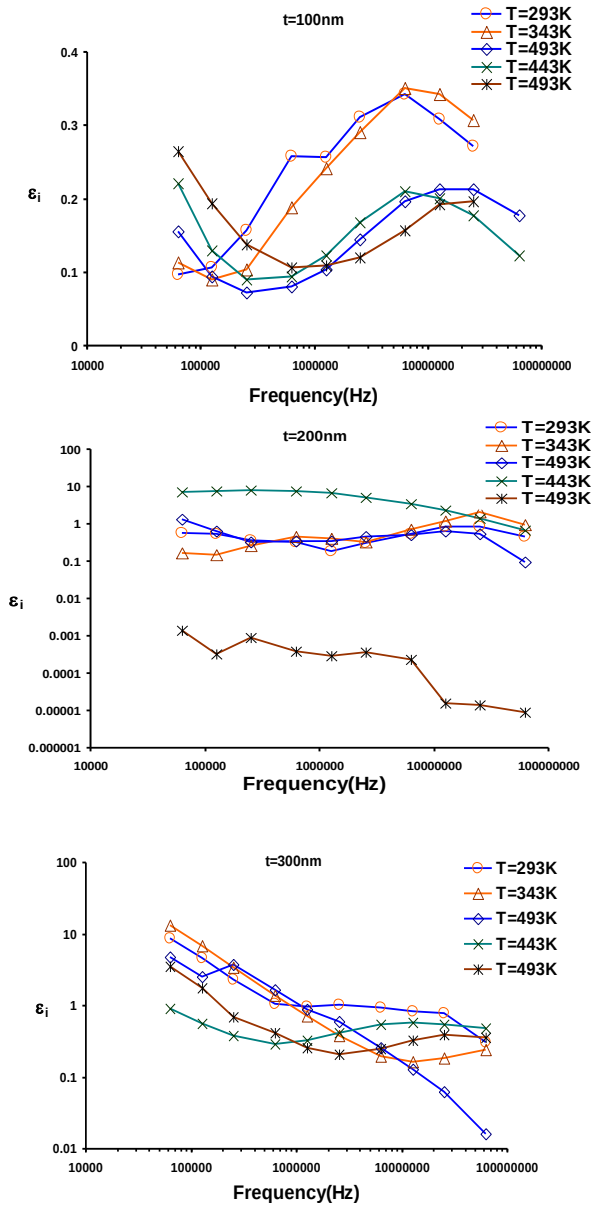

Fig.7 Variation of imaginary part of permittivity (ε_i) with frequency of SnS films with different thicknesses and temperatures

The temperature dependence of real dielectric constant ε_r at different fixed frequencies over the temperature range of 293-493K of SnS films with different thickness is shown in Fig. 6. A broad dielectric peak near 440K and 340K for thickness 100, 200 and 300 nm respectively is attributed to the phase transition temperature from zinc blend to orthorhombic structure (David Avellaneda *et al*, 2009). It is obvious that the transition temperature decreases with the increase of thickness.

It is useful to distinguish long-range conduction process from the localized dielectric relaxation. To visualize this, we have plotted the imaginary part of complex dielectric permittivity ε_i as a function of frequency for SnS films with different thicknesses as representatives Fig. 7. Dielectric relaxation is a result of the reorientation process of dipoles, which show a peak in ε_i spectra. For SnS samples with higher ion concentration, the movement of ions from one site to another will perturb the electric potential of the surroundings. Motion of the other ions in this region will be affected by perturb potential. Such a cooperative motion of ions will lead to non-exponential decay, or a conduction processes with distribution of relaxation time (Y. Fu, K. Pathmanathan *et al*, 1991). It has been observed that (Figure 7) in the imaginary part of dielectric spectra, a relaxation peak is observed for the ε_i for lower thickness i.e. t=100nm , whereas no well pronounce peak is observed in the dielectric spectra for higher thicknesses. This suggests that charge motion strongly coupled manifesting as a single peak in the ε_i spectra with no corresponding feature in dielectric spectra for higher thicknesses (P. Jeevanandam *et al,* 1998).

So the conduction takes place through charge migration of ions between coordinated sites of along with the segmental relaxation of semiconductor. An enhanced of conduction is a natural consequence of thickness increment. The higher value of dielectric loss ε_i at low frequency is due to the free charge motion within the materials. On thickness increment ε_i increases in the lower frequency region reflect the enhancement of mobility of charge carrier.

As the temperature increases ε_i first decreases with rise in frequency in low frequency region followed by a peak in the loss spectra. The loss peak for lower thickness is shifting towards the higher frequency side with the increase of temperature while loss peak is shifting towards the lower frequency side with the increase of temperature for higher thicknesses. The appearance of peak is attributed to the relaxation phenomena. Similar types of observations have been reported in literature (F. Kremer *et al,* 2003; M. Marzantowicz *et al*, 2006). It is generally believed that dielectric data is characterized by superposition of two processes: conductivity contribution that produces an increase of both real part ε_r and the imaginary part ε_i of the dielectric function on decreasing frequency and a relaxation process exhibiting a maximum in ε_i that shifts higher frequency side with increase in temperature. The measured dielectric loss ε_i spectrum contains contribution from two sources: dipolar orientation and diffusion of charge carrier. When interfacial polarization occurs thickness resulted in overall increase of ε_r and ε_i due to free charge contributions. So the increase of the molecular mobility is reflected both by increase of free charge mobility and the shift of the peak towards the higher frequency side with simultaneous increase of its magnitude (Fig. 6). The overall result is enhancement of conductivity on thickness increment.

A direct evidence of the existence of multi-relaxation time in the as-deposited SnS films treated at temperature in the range from 293 to 493 K is obtained by plotting Cole–Cole diagrams as shown in Figure 8. It has been observed that as thickness increases, ε_r versus ε_i curves represent the arc of circles having their centers lying below the abscissa axis will be vanished. This confirms the existence of the distribution of τ in for lower thickness films. By measuring the angles ($\alpha\pi/2$) the values of the polarizability (α) have been determined and were listed in table 3. We can note that the values of α declares a non systematic variation with the increase of thickness and thermal treatment temperature. However, in general α tends to increase with thermal treatment temperature. This is in agreement with the concept of molecular relaxation; the increase of α value results from the reduction of the forces as a result of the formation of the barrier between quaternary elements, while the decrease of α with the increase of heat treatment results from the rise of the forces of the intermolecular, i.e. α increases from 0.133 to 0.277 when T increases from 293 to 343 K while α decreases from 0.222 to 0.055 when the temperature of thermal treatment T increases from 443 to 493 K for samples with thickness 100nm (Srivastastava *et al,* 1979; El Anwar *et al*, 1999).

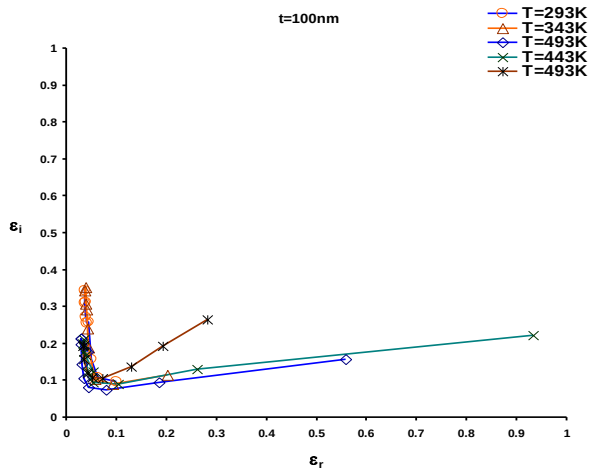

Fig.8 Cole – Cole diagrams of SnS films for different temperatures

3.1.2 Photoconductivity of SnS thin films

The SnS thin films show n-type conductivity in the first converts to p-type conductivity with thickness increasing using Hall Effect. A layer of aluminum electrode is deposited on the films in order to measure the conductivity, and then the related parameters are recorded by a Keithley. The halogen tungsten lamp with a light intensity of 106mW/cm^2 is used as the light source to measure the photo conductivity. The dark conductivity σ_d and photo conductivity σ_{ph} at various thickness are obtained (shown in table 5). The dark conductivity of the films increases with the thickness increasing. It should be noticed that the conductivity is 3.7x10^{-5} (Ω.cm)$^{-1}$ at thickness 100nm increases to 9.44x10^{-4}(Ω.cm)$^{-1}$ with thickness increasing. The low conductivity of SnS films grown at low thickness is due to the low grain size and the poor crystallinity of the SnS films. When the thickness is 300nm, the preferential orientation of the film becomes significant. The variation of the ratio of σ_d/σ_{ph} is low since more photon-induced carriers will recombine because of the abundant internal defects in the films deposited at low thickness, which consequently reduces the ratio of σ_d/σ_{ph} of the films, which increases with increase of thickness and reach maximum at thickness 300nm because the film has the best crystallinity and the largest grain size compared with the samples deposited at other thickness.

Table 5 Dark-conductivity and photoconductivity of SnS thin films

Thickness (nm)	σ_d(Ω·cm)$^{-1}$	σ_{ph}(Ω·cm)$^{-1}$	σ_{ph}/σ_d
100	3.720x10^{-5}	7.07x10^{-5}	1.9
200	7.751x10^{-5}	0.000217	2.8
300	9.442x10^{-4}	0.00472	4.5

Conclusions

SnS thin films have been prepared at different thickness (100 ,200, and 300nm) by vacuum evaporation. Experimentally, the properties of the SnS films depend on the thickness significantly. When the thickness is 300nm, SnS thin films are polycrystalline with orthorhombic structure and the preferential orientation appears along the plane (111)and a stoichiometric ratio of Sn/S approaching 1 .maximum dark conductivity and photo conductivity of the film is 8.33x10^{-5}(Ω·cm)$^{-1}$and 2x10^{-4}(Ω.cm)$^{-1}$, respectively.

Slope values (s) of SnS films show progressive decrease with thickness. The conductivity is pure ac for lower thickness, while the conductivity is frequency independent for high thickness. The increase of SnS thickness causes the proceeding reduction of s, i.e. increases the d.c conductivity . The increase of thickness leads to reduces the values of polarisability of SnS films consequently increases the intermolecular force ,while increase of temperature reduces the force of the intermolecular through out formation a barrier.

Acknowledgments

The Authors wish to thank the Department of Physics /College ofw Science/University of Baghdad for supporting this work.

References

J. B. Li, V. Chawla, and B. M. Clemens (2012), Investigating the role of grain boundaries CZTS and CZTSSe thin filn solar cell with scaning probe microscopy, *Adv. Mater*., 24, pp.720-23.

P. P. Choi, O. C. Miredin, and R. Wuerz (2012), *Surf. Interface Anal*., 44, pp.1386.

J. J. Scragg, P. J. Dale, D. Colombara, and L. M. Peter (2012), Thermodynamic aspects of the synthesis of thin films materials for solar cells, *ChemPhysChem*., 13, pp.3035.

L. Grenet, S. Bernardi, D. Kohen, C. Lepoittevin, S. Noel, N. Karst et al (2012), Cu $_2$ ZnSn (S $_{1-x}$ Se $_x$) $_4$ based solar cell produced by selenization of vacuum deposited precursors*, Solar Energy Materials and Solar Cells* ,101, pp.11-14

L. Price, I.P. Parkin, A.M.E. Hardy, and R.J.H Clark et al (1999), Atmospheric Pressure Chemical Vapour Deposition of Tin Sulfides (SnS, Sn $2S_3$, SnS_2) on glass, Chem, *Mater.*, 11, pp.1792-1799.

K.T. Ramakrishna, P. Purandar (2002), Structural studies on SnS films grown by a two-stage process, *Materials Letters*, 56, pp.108-111.

K. Takeuchi, M. Ichimura, E. Arai, and Y. Yamazaki (2003), SnS thin films fabricated by pulsed and normal electrochemical deposition, *Solar Energy Mater. and Solar Cells*, 75, pp.427-432.

A. K. Jonscher (1983), *Dielectric Relaxation in Solids*, Chelsea Dielectric Press, London.

A. K. Jonscher (1977), The 'universal' dielectric response *Nature,* 267 pp.673-679.

K. A. Mauritz (1989), dielectric relaxation studies of ion motions in electrolyte containing perfluorosulfonate*, Macromolecules,* 22, pp. 4483-88.

K. P. Singh and P. N. Gupta (1998), Study of dielectric relaxation in polymer electrolytes, *European Polymer Journal,* 34(7), pp.1023-29.

S. Ramesh, A. H. Yahaya and A. K. Arof (2002), Dielectric behaviour of PVC-based polymer electrolytes,"Solid State Ionics, *Solid State Ionics,* 152-153 pp.291-294.

B. Natesan, N. K. Karan and R. S. Katiyar (2006), Ion relaxation dynamics and nearly constant loss behavior in polymer electrolyte, *Phys. Rev. E,* 74(4 Pt 1), 042801.

David Avellaneda, M.T.S. Nair, P.K. Nair (2009), Photovoltaic structures using chemically deposited tin sulfide thin films, *Thin Solid Films*, 517,pp. 2500–2502

Y. Fu, K. Pathmanathan and J. R. Steven (1991), *J. Chem. Phys.* ,94, pp.6326.

P. Jeevanandam and S. Vasudevan (1998), Arrhenius and non-Arrhenius conductivities in intercalated polymer electrolytes*, J. Chem. Phys.,* 109, pp. 8109-17.

F. Kremer and A. Schonhals (2003) (Eds.), *Broad Band Dielectric Spectroscopy*, Springer-Verlag Berlin Heidelberg, New York.

M. Marzantowicz, J. R. Dygas, F. Krok, Z. Florjanczyk and E. Zygadlo-Monikowska (2006), Influence of crystallization on dielectric properties of PEO:LiTFSI polymer electrolyte,, *J. Non-Crystalline Solids,* 352(42), pp.5216-23.

Srivastastava K K, Kumar A, Panwar O S and Lakshminarayan K N (1979), Dielectric relaxation study of chalcogenide glasses, *J. Non-Cryst. Solids,* 33(2) 205-224.

El Anwar I M, Mohamad A K and Hammad F F (1999), Some dielectric properties of strontium titanate doped with some metal oxides*, Egypt.J. Chem.* 42(6), pp. 527–54 4.